

# **Design Optimization Study on the Single Tank Packed-bed Thermal Energy Storage System**

Jun Soo Yoo

November 2018



The INL is a U.S. Department of Energy National Laboratory  
operated by Battelle Energy Alliance

# **Design Optimization Study on the Single Tank Packed-bed Thermal Energy Storage System**

**Jun Soo Yoo**

**November 2018**

**Idaho National Laboratory  
Idaho Falls, Idaho 83415**

**<http://www.inl.gov>**

**Prepared for the  
U.S. Department of Energy**

**Under DOE Idaho Operations Office  
Contract DE-AC07-05ID14517**

# DESIGN OPTIMIZATION STUDY ON THE SINGLE TANK PACKED BED THERMAL ENERGY STORAGE SYSTEM

**Junsoo Yoo<sup>\*</sup>, Su-Jong Yoon, Thomas E. O'brien, Konor L. Frick, James E. O'brien, Piyush Sabharwall and Carl M. Stoots**

Idaho National Laboratory

<sup>\*</sup>junsoo.yoo@inl.gov

sujung.yoon@inl.gov; thomas.obrien@inl.gov; konor.frick@inl.gov; james.obrien@inl.gov; piyush.sabharwall@inl.gov; carl.stoots@inl.gov

## ABSTRACT

Idaho National Laboratory (INL) is establishing the Dynamic Energy Transport and Integration Lab (DETAIL) as part of its commitment to research on nuclear-renewable hybrid energy systems and associated advanced reactor technologies. DETAIL is designed to allow several different energy systems to work in unison. Current plans include a PWR simulator, high-temperature steam electrolysis (HSTE) unit, and a renewable energy system (e.g., photovoltaics). DETAIL will provide the real world basis for studies on the systems integration and system configurations to be completed. Encompassed in the DETAIL program is the Thermal Energy Storage (TES) system. The TES system is one of the key components in DETAIL because it allows for the delayed release of energy and can be used to simulate storage capabilities currently being considered by utility providers. Of the various TES concepts, this paper deals with the single-tank packed bed TES system. Particular attention is given to the transient thermal behavior of fluid and solid particles within the packed bed thermocline tank and heat storage efficiency influenced by various design parameters. The effects of tank geometry (height-to-diameter ratio), filler size, filler packing ratio and operating temperature differentials are investigated. Based on the parametric study and cost analysis, the optimal TES tank design for DETAIL is discussed.

## KEYWORDS

Packed-bed Thermal Energy Storage, Nuclear-Renewable Hybrid Energy System, Heat Storage Efficiency

## 1. INTRODUCTION

As renewable energy technologies improve in efficiency and price-point, renewables such as wind and solar energy are becoming more attractive energy resources. However, increasing the penetration of renewables on the electric grid is challenging because the inherent variability can significantly stress an already aging grid. A proposed solution is to integrate base load plants such as nuclear power plant with renewables into a single hybrid energy system. At Idaho National Laboratory the Nuclear-Renewable Hybrid Energy System (N-R HES) program was created to study the inclusion of carbon free renewables with the main carbon free base load plant [1]. This program has shown that excess energy resulting from the energy generation-demand imbalances can be reserved for future use (e.g., for the periods of excess demand) or switched to other industry needs (e.g., H<sub>2</sub> production, desalination). Program results imply that integration of base load plants and intermittent energy resources can address grid flexibility and carbon emission concerns while still producing attractive economic returns.

To further substantiate the N-R HES simulations, Idaho National Laboratory is establishing the Dynamic Energy Transport and Integration Lab (DETAIL) [1] project. The proposed system configuration is shown in Fig. 1. Various experimental and analytical studies on system integration, dynamic control, thermal energy storage/delivery, heat exchanger performance, etc. will be performed for model validation, model development, and ultimately system deployment purposes of the overarching N-R HES program [3].

As of July 2018 development has been focused on the Thermal Energy Delivery System (TEDS) that will be installed in DETAIL. TEDS is the backbone of the system since it is the primary way heat is transferred from system to system. Due to its relative importance, TEDS is designed with configurability, controllability, and measurability in mind. As part of those considerations a thermal storage unit will be installed within TEDS. This will allow for system maneuverability and flexibility that simply would not be possible otherwise. Thermal Storage comes in many varieties and is specific to the application. However, DETAIL, by its very definition, requires flexibility. Accommodating such a requirement quickly eliminates many forms of thermal storage. The remaining popularized forms of thermal energy storage were: two-tank single fluid, two-tank packed bed, single fluid thermocline, and packed bed thermocline.

Taking both the cost and heat storage efficiency into account, the packed bed thermocline system was chosen. To determine optimal TES design parameters thermal modeling and analysis was required. The numerical models and results of which are presented below.

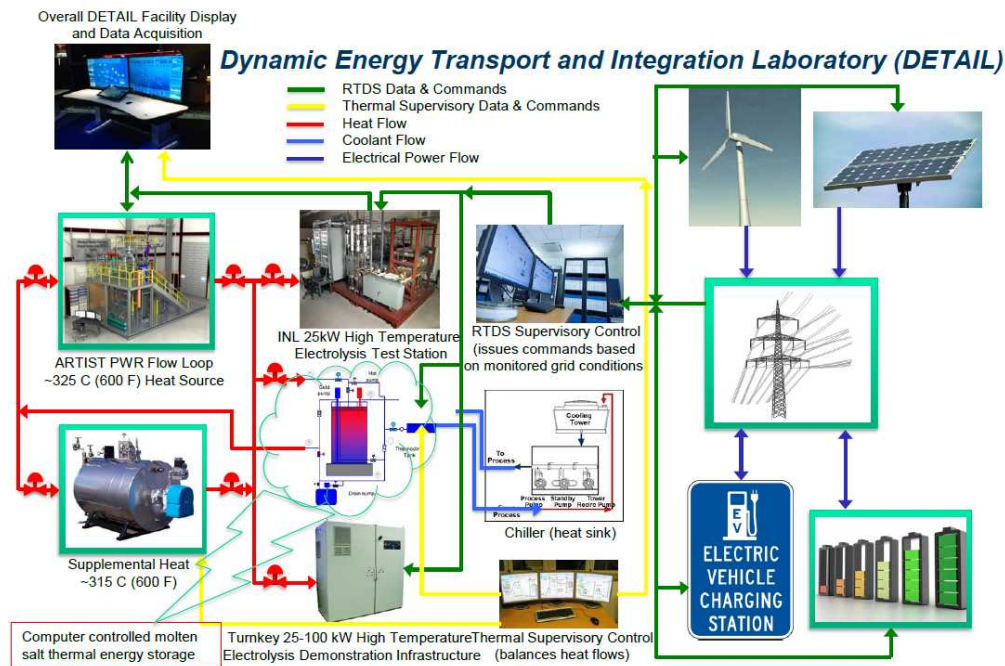


**Fig. 1. System Configuration of Dynamic Energy Transport and Integration Laboratory (DETAIL)**  
[1]

## 2. NUMERICAL MODELING OF THERMAL ENERGY STORAGE SYSTEM

### 2.1 Design Parameters for Thermal Energy Storage (TES) tank

Major design parameters for the packed bed TES tank are tabulated in Table 1. Considering the high volumetric capacity and well-defined material characteristics, alumina ( $\text{Al}_2\text{O}_3$ ) is adopted as heat storage medium (i.e., filler material). Alumina has been considered as a favorable heat storage medium in the literature [2, 3]. It has a high volumetric heat capacity of about  $3046 \text{ kJ/m}^3$  which is higher than many other materials commonly used for packed bed thermal storage system, such as a brick, soil, sandstone, rocks, concrete, granite, etc. The size of filler will be in range from 1/8" to 5/8". The packing ratio considered is ranged from 0.58 to 0.70. The operational temperature differential of a storage tank under consideration is in the range of  $50^\circ\text{C}$  to  $150^\circ\text{C}$ . The TES tank size was determined to achieve the maximum heat storage capacity of 200 kWh.

**Table 1. Design parameters considered for the present study**

Design parameters	
Heat transfer fluid (HTF)	Therminol-66 [4]
Maximum heat storage capacity	200 kWh
$T_{\text{high}}$ (hot fluid temperature)	$325^\circ\text{C}$
$\Delta T (= T_{\text{high}} - T_{\text{low}})$	$50\text{--}150^\circ\text{C}$
Filler material	Alumina [5]
Filler material size (diameter)	1/8"–5/8"
Porosity (packing ratio)	0.3–0.42 (0.58–0.70)

Therminol-66 is the chosen heat transfer fluid (HTF) for TEDS. The hot fluid of  $325^\circ\text{C}$  from water loop (PWR simulator) will be a heat source for the TEDS. Therminol-66 can be operated at up to  $345^\circ\text{C}$  without phase change. The vapor pressure of Therminol-66 at  $325^\circ\text{C}$  is 52.5 kPa (7.6 psi). Readers are advised to refer to Ref. [4] for the detailed thermo-physical properties of Therminol-66.

### 2.1. Governing Equations and Numerical Method

Thermal Energy (or heat) Storage (TES) system can be classified into three different types: (i) sensible, (ii) latent and (iii) thermo-chemical, all with their own advantages and disadvantages. The poison of choice for TEDS is sensible-heat. Sensible heat thermal storage is achieved without phase change and instead simply takes advantage of a materials heat storage capabilities when heated to a higher temperature.

A disadvantage of packed bed thermoclines is the degradation in exit temperatures and system efficiency that occurs over system discharge. This is because as the thermocline moves within the tank, heat removal from the packed bed begins to reduce. To model such behavior the Schumann's equations are widely used. The Schumann's energy equations have been successfully used and validated against experimental data obtained from packed bed TES systems [6, 7]. The equations are given as:

$$\frac{\partial T_f}{\partial t} + U_f \frac{\partial T_f}{\partial z} = \frac{h S_s}{(\rho_f C_{p,f}) \varepsilon \pi R^2} (T_s - T_f) \quad (\text{for fluid}) \quad (1)$$

$$\frac{\partial T_s}{\partial t} = - \frac{h S_s}{\rho_s C_{p,s} (1 - \varepsilon) \pi R^2} (T_s - T_f) \quad (\text{for filler material or solid particles}) \quad (2)$$

where  $t$  is the time,  $z$  is the position along a tank in the direction of fluid flow,  $C_{p,f}$  and  $C_{p,s}$  are the specific heat of fluid and solid, respectively,  $T_f$  and  $T_s$  are the fluid and solid temperature, respectively,  $\rho_f$  and  $\rho_s$  are the fluid and solid particles density, respectively,  $U_f$  is the fluid velocity,  $\varepsilon$  is the porosity,  $h$  is the heat transfer coefficient,  $S_s$  is the heat transfer surface area per unit length (height) of a tank, and  $R$  is the radius of a storage tank.

In formulating the equations (1) and (2), the following assumptions are applied:

- (i) Uniform fluid flow exists throughout the storage tank,
- (ii) No radial thermal gradient exists across the storage tank (i.e., 1-D modeling),
- (iii) Storage tank is ideally insulated (i.e., adiabatic boundary condition),
- (iv) No thermal gradient in the solid particles exists (lumped capacitance method),
- (v) Conductive heat transfer in the fluid and between the solid particles is neglected.

Therefore, to ensure the fidelity of modeling results, modeling conditions should be first checked with proper dimensionless parameters such as *Pecel number* and *Biot number*.

In order to obtain the numerical solution for the equations (1) and (2) coupled each other, the numerical method proposed by Lew et al. [8], which is based on the method of characteristics, was employed. This numerical scheme provides fast, efficient, and accurate algorithm to solve the equations (1) and (2) without the need of iterative solver. To apply this numerical scheme, the governing equations should first be reduced to dimensionless form by introducing the following dimensionless parameters:

$$\theta_f(z, t) = \frac{T_f(z, t) - T_{low}}{T_{high} - T_{low}} \quad (\text{Dimensionless temperature of fluid}) \quad (3)$$

$$\theta_s(z, t) = \frac{T_s(z, t) - T_{low}}{T_{high} - T_{low}} \quad (\text{Dimensionless temperature of solid particle}) \quad (4)$$

$$z^* = z / H \quad (\text{Dimensionless position}) \quad (5)$$

$$t^* = t / (H / U) \quad (\text{Dimensionless time}) \quad (6)$$

Then, the dimensionless form of the Schumann equations [equations (1) and (2)] is derived as follows [8]:

$$\frac{\partial \theta_f}{\partial t^*} + \frac{\partial \theta_f}{\partial z^*} = \frac{1}{\tau_s} (\theta_s - \theta_f) \quad (7)$$

$$\frac{\partial \theta_s}{\partial t^*} = - \frac{H_{CR}}{\tau_s} (\theta_s - \theta_f) \quad (8)$$

where  $\tau_s = \frac{U_f}{H} \frac{\rho_f C_{p,f} \varepsilon \pi R^2}{h S_s}$ ,  $H_{CR} = \frac{\rho_f C_{p,f} \varepsilon}{\rho_s C_{p,s} (1 - \varepsilon)}$  and .

Note that the dimensionless energy balance equations (7) and (8) can be solved along the characteristic [9], allowing the equation (7) to be further reduced along the characteristic  $t^* = z^*$  as follows:

$$\frac{D\theta_f}{Dt^*} = \frac{1}{\tau_s} (\theta_s - \theta_f) \quad (9)$$

The dimensionless form of equations (8) and (9) are the linear system of hyperbolic type equations and hence, the numerical solution can be directly obtained without relying on the iterative solver if the properties of fluid and packed bed solid particles are assumed constant.

## 2.2. Modeling Scenario, Code Verification, and Additional Modeling Features for Design Optimization Study

The thermocline heat storage tank works alternatively between two different operating modes: discharge and charge modes (see Fig. 2). During the discharge mode, the hot fluid ( $T_{high}$ ) is discharged from the top of a tank while the cold fluid is charged from the bottom to keep the same volume of fluid inside the tank. Conversely, during the charging process the hot fluid ( $T_{high}$ ) is charged to the tank from the top while the cold fluid ( $T_{low}$ ) is discharged from the bottom. Since the hot and cold fluids coexist in the tank as shown in Fig. 2, the temperature of hot fluid flowing out of the tank during the discharge mode may decrease with time as the pre-existing hot fluid is discharged. The thermal modeling of heat storage tank is conducted by considering these operating principles. It is noted that evaluating and understanding the heat storage efficiency is important when designing the thermocline tank. One of the most common ways to estimate heat storage efficiency is based on the following equation [8]:

$$\eta_{eff} = \frac{\int_0^{t_{disch}} m C_{p,f} [T_{f,out}(t) - T_{low}] dt}{\int_0^{t_{ch}} m C_{p,f} (T_{high} - T_{low}) dt} \quad (10)$$

(where  $T_{f,out}(t)$  is the temperature of fluid discharged from the top of a tank (outlet) at time  $t$ ,  $t_{disch}$  is the discharge time period,  $t_{ch}$  is the charge time period.)

Another way to assess heat storage efficiency is to calculate exergy efficiency  $\eta_{exergy}$  [10] which accounts for the temperature level at which the energy is charged or discharged during operation:

$$\eta_{exergy} = \frac{\Xi_D}{\Xi_C} = \frac{\int_0^{t_{disch}} [\{T_f(H_{tank}) - T_0\} - T_0 \cdot \ln(\frac{T_f(H_{tank})}{T_0})] dt}{[(T_{high} - T_0) - T_0 \cdot \ln(\frac{T_{high}}{T_0})] \cdot t_{ch}} \quad (11)$$

(where  $\Xi_C$  is the charged exergy,  $\Xi_D$  is the discharged exergy,  $T_0$  is the reference temperature,  $T(H_{tank})$  is the fluid temperature coming from the top the TES tank during a discharge mode.)

It is noted that the design study presented below was carried out based solely on Eq. (10) and the results were comparable with those estimated by Eq. (11) in the present work.

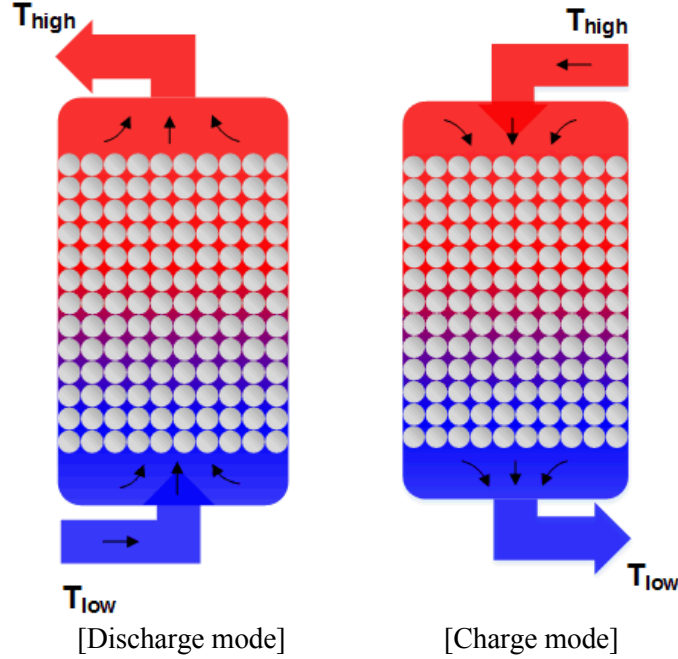


**Fig. 2. Flow path of hot and cold fluid across the thermocline TES tank during discharge and charge modes**

Once the code was established based on the numerical scheme described in Section 2.1, the code verification was performed by comparing the results with those presented by Lew et al. [8] which has already been verified with several analytical solutions. Fig. 3 shows that the present code can reproduce the same fluid temperature profile with those obtained from the already verified code simulation. In the present code, additional algorithm was implemented to consider the temperature-dependent properties of HTF (i.e., Therminol-66) and filler material (i.e., alumina) since the properties of these materials change substantially within the operating temperature range of our interest (i.e., about 200-330 °C). The difference of modeling results, however, was insignificant as shown in Fig. 4. Finally, the modified version of Ergun equation proposed by Zanganeh et al. [11] was implemented for the present design optimization study, which allowed us to estimate the pressure drop through the packed bed. This is to determine if the main circulation pump installed in TEDS loop can operate properly after considering the pressure drop produced by the TES tank.



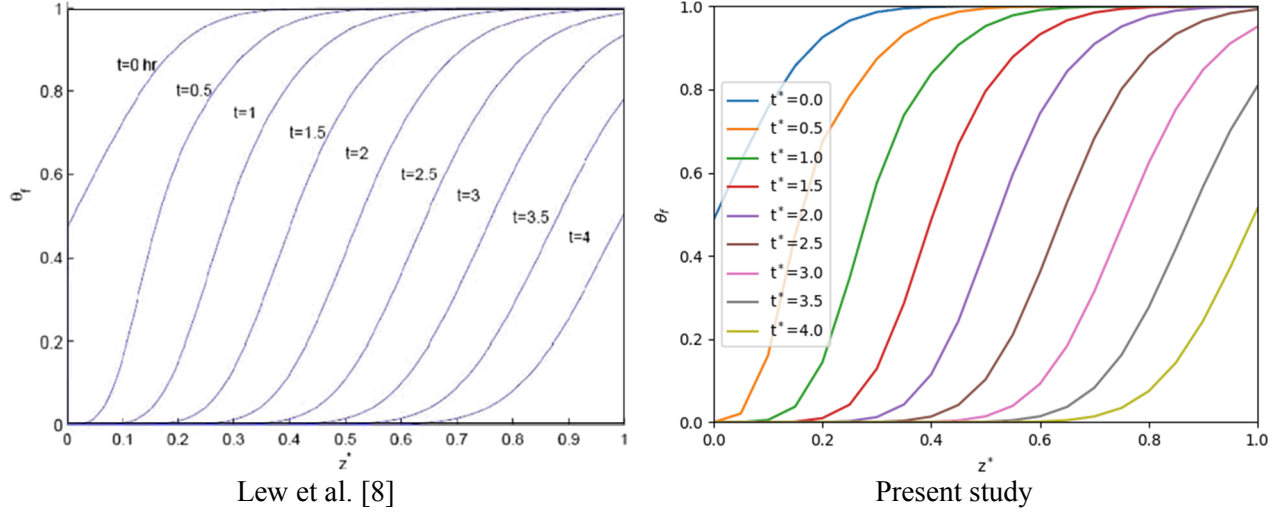


**Fig. 3. Code-to-Code Comparison for Code Verification (Transient Temperature Profile within the Thermocline TES Tank under the Same Modeling Condition)**

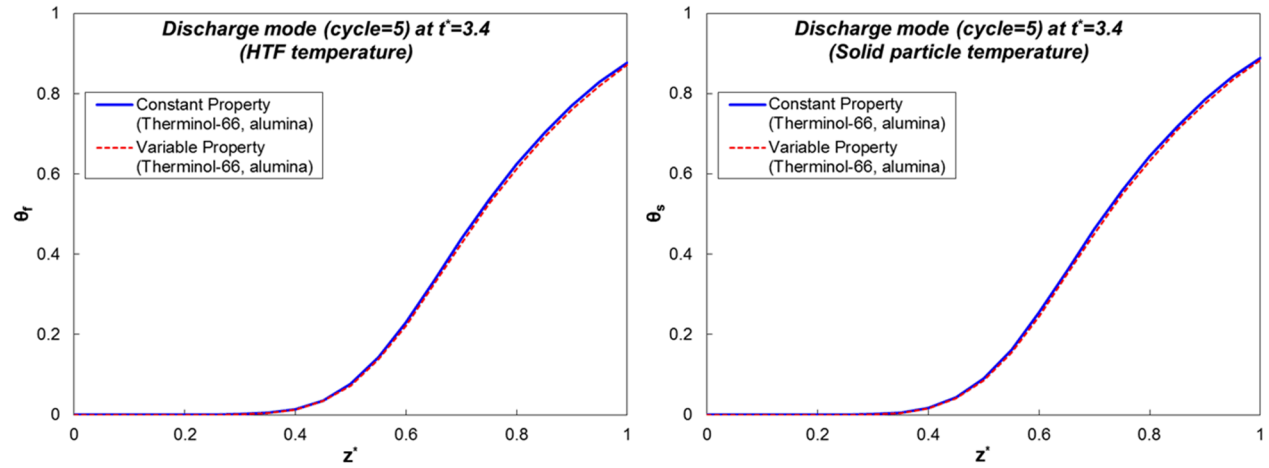


**Fig. 4. Effect of considering temperature-dependent fluid and filler material properties**

### 3. RESULTS AND DISCUSSION

#### 3.1. Problem Set-up and Grid Independence Study

The base case study was conducted to determine the reference design parameters of thermocline TES system. The base case was selected in consideration with requirements of co-located systems. The heat transport fluid is Therminol-66 and filler material is alumina. The thermal storage capacity is 200 kWh and the hot temperature of fluid is 325°C and operating temperature differential is 50 °C. Base storage tank diameter is 1.2m and height-to-diameter ratio is 2.9. Porosity of the packed bed is assumed to be 0.3.

To determine the proper grid size that can be used for present design optimization study, a grid sensitivity study was conducted for the base case described above. The number of nodes for the storage tank volume was tested from 10 to 40 by twice increment. During this test, it was found that the time-dependent temperature profiles across the thermocline tank were converged as it reached the 15<sup>th</sup> cycle of discharge and charge mode (note that one cycle consists of a pair of discharge and charge modes). Fig. 5 shows the grid sensitivity results for the discharge and charge modes, which are the case after the temperature

profiles are converged at the 15<sup>th</sup> cycle. The grid sensitivity results showed that the number of grid has no significant effect on the results. The present code runs fast even with the finest nodes. To ensure the accurate numerical solution in any case, the following parametric studies described in the Section 3.2 were performed with 40 nodes. Trapezoidal rule was applied to numerically integrate the Eqs. (8) and (9), which leads to the formal accuracy of  $O(\Delta t^{*2})$  [8].

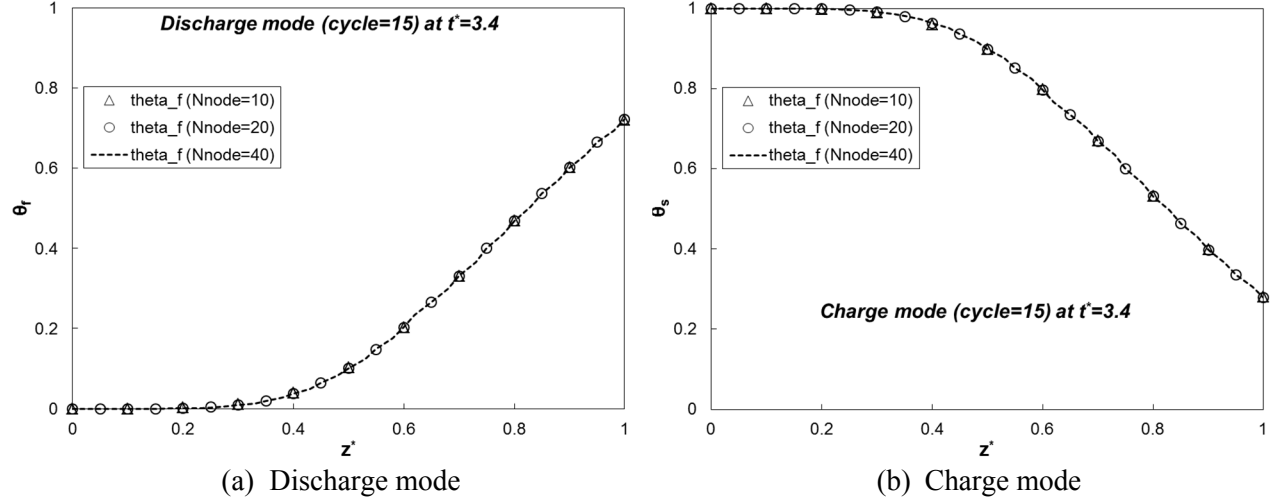
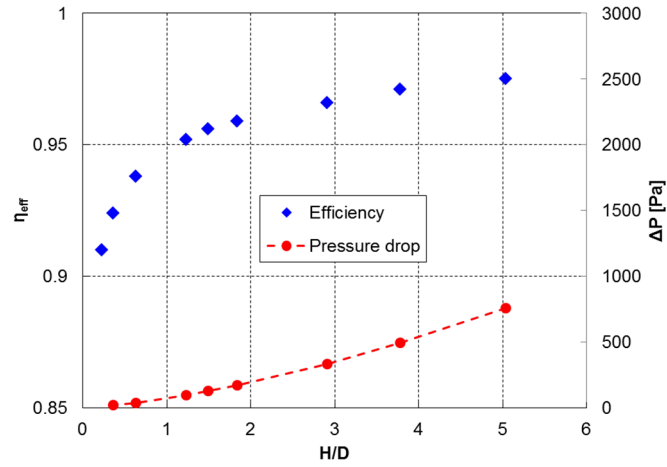


**Fig. 5. Grid sensitivity results on both discharge and charge modes**

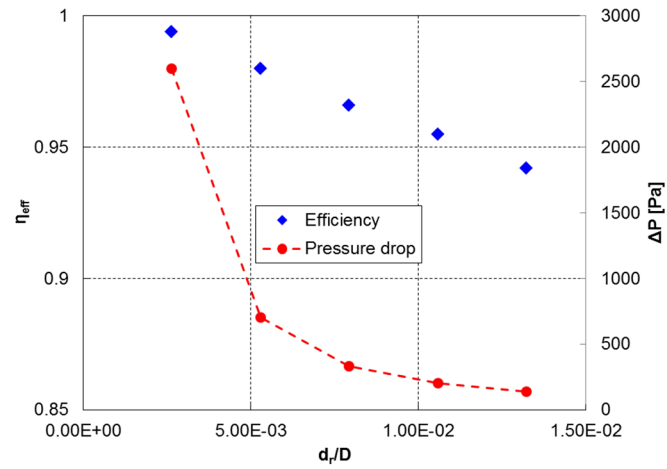
### 3.2. Parametric Study and Discussion

To determine the optimal TES tank design for DETAIL, effects of various design parameters on the heat storage/delivery efficiency as well as the overall cost were investigated. The design parameters of present interest include tank geometry (i.e., height-to-diameter ratio), filler (or packed bed solid particle) size, porosity (or packing ratio), and operating temperature differential (i.e.,  $\Delta T = T_{\text{high}} - T_{\text{low}}$ ). In addition, the pressure drop is also evaluated because those design parameters can substantially influence the flow resistance through the packed bed storage tank. The thermocline TES tank has once-through system. Hence the pressure drop through the storage tank increases with the increase of height-to-diameter ratio ( $H/D$ ) as shown in Fig. 6-(a). Fig. 6-(a) also shows that the heat storage efficiency [ $\eta_{\text{eff}}$ , see Eq. (10)] increases logarithmically with  $H/D$ . This is because given the same tank volume and mass flow rate, the heat transfer fluid flows through the narrower passage (i.e., higher  $H/D$ ) at higher speed, causing the higher heat transfer rate between the fluid and heat storage media (i.e., fillers). Also, it was seen that the thermal gradients along the fluid flow through the tank decreased as the  $H/D$  increased. Note that in the two-tank storage systems [12], which stores the hot and cold fluids separately, the flat geometry of tank ( $H/D < 1$ ) is often employed because there is less concern of temperature degradation (or heat storage degradation) within the storage tank. For the other parametric studies discussed below, the height-to-diameter ratio ( $H/D$ ) of 2.9 was used as a reference value.

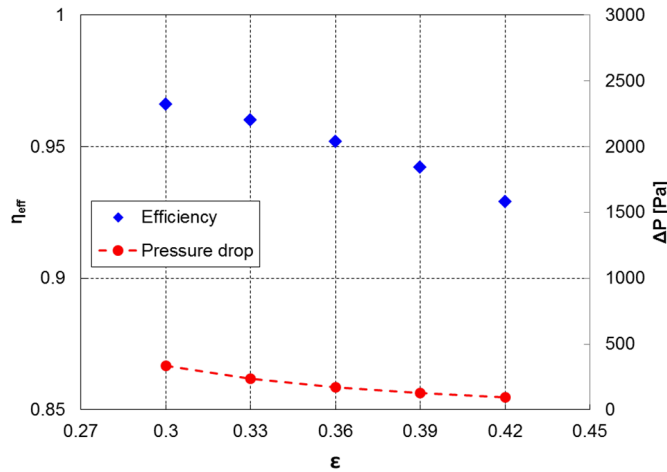
Fig. 6-(b) shows the effect of filler size. The size of filler shows substantial influence on the heat storage efficiency as well as the pressure drop. The efficiency of heat storage decreased from 0.98 to 0.94 by increasing the ratio of filler diameter ( $d_f$ ) to tank diameter ( $D$ ). This is because the smaller filler diameter ensures the larger heat transfer area between the heat transfer fluid and heat storage media (fillers). Fig. 6-(b) also shows that the pressure drop through the storage tank increased exponentially as the filler size (the ratio of  $d_f/D$ ) decreased. Taking the cost of alumina (filler), heat storage efficiency, and pressure drop into account, the optimal filler diameter was determined to be  $1/8''$ .



(a) Tank geometry ( $H/D$ ) effect



(b) Filler size ( $d_r/D$ ) effect



(c) Porosity ( $\epsilon$ ) effect

**Fig. 6. Results of Design Parameter Study**

It is noted that considering the characteristic of the main circulation pump under consideration for TEDS, it turned out that the pressure drop was not the limiting factor. It is also important to mention that the amount of effectively recoverable energy from the TES tank (i.e., bed utilization factor) increased significantly by adopting the smaller size of filler material. In Fig. 6-(c), we also investigate the effect of porosity of the packed bed storage tank. Considering the typical porosity ( $\epsilon$ ) range of the packed bed heat storage systems in the literature, the parametric study was performed for the range of  $\epsilon$  between 0.3 and 0.42. Given the fixed tank volume and H/D, the higher value of  $\epsilon$  decreased the heat storage efficiency. This is because by increasing the porosity, the volume of alumina (filler) that have the higher volumetric heat capacity than the fluid (i.e., Therminol-66) was decreased within the heat storage tank.

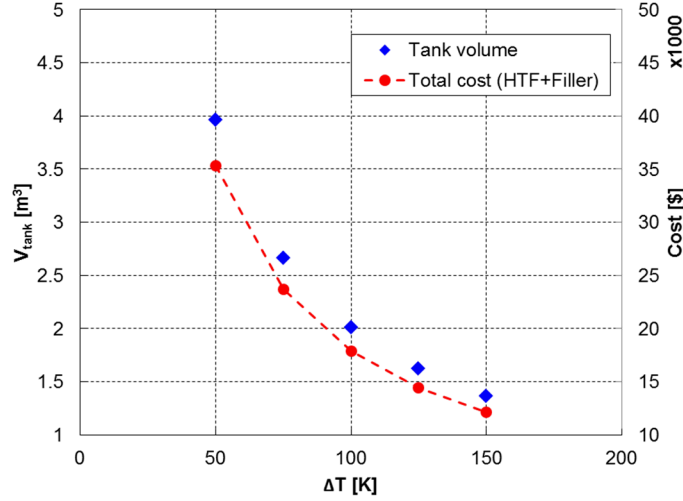


**Fig. 7. Effect of Operating Temperature Differential on the Required Tank Volume and Cost**

Lastly, the effect of operating temperature differential  $\Delta T$ , which is defined by the fluid temperature difference between  $T_{\text{high}}$  ( $=325^\circ\text{C}$ ) and  $T_{\text{low}}$ , is shown in Fig. 7. Given the mass flow rate of fluid (Therminol-66), the larger  $\Delta T$  allows the higher energy storage density. This means that the total volume of a tank can be reduced to store the same amount of energy by increasing the  $\Delta T$ . Therefore, considering the high cost of heat transfer fluid, the  $\Delta T$  can help significantly reduce the overall cost of TES system as shown in Fig. 7. It is noted that in Fig. 7 we only consider the cost of Therminol-66 and alumina, but not the cost of the storage tank. Fig. 7 shows the estimated cost (HTF + alumina) as well as the required tank volume to attain the target heat storage capacity of 200 kWh at different  $\Delta T$ . The operating temperature differential  $\Delta T$  showed little effect on the heat storage efficiency. Considering the budget, heat storage efficiency, temperature requirement for the applications of interest (e.g., high-temperature electrolysis for  $\text{H}_2$  production), and heat delivery time, the operating temperature differential of about  $100^\circ\text{C}$  was determined as an optimal value.

#### 4. SUMMARY AND CONCLUSIONS

The optimal design of thermal energy storage tank that can be applied to DETAIL was studied through the thermal analysis of packed-bed thermocline tank. For thermal modeling, the numerical model to solve the Schumann's energy equations was established based on the numerical method proposed by Lew et al. [8]. After verifying the numerical model (or code), some improved features were added for the present design study, specifically to consider the temperature-dependent material properties and pressure drop through the packed bed. Then, the parametric study was performed with various design parameters, i.e., tank geometry (height-to-diameter ratio), filler size, porosity, and operating temperature differential.

Considering the budget, thermal storage design target (e.g., heat storage capacity), and analysis results, the optimal design of the thermal energy storage tank was discussed.

## ACKNOWLEDGMENTS

This work was supported by Department of Energy Office of Nuclear Energy. Idaho National Laboratory is operated for the United States Department of Energy Office of Nuclear Energy by Battelle Energy Alliance, LLC, under contract No. DE-AC07-05ID14517.

## REFERENCES

1. O'Brien, J.E., et al., *High-Pressure, High-Temperature Thermal Hydraulic Test Facility for Nuclear-Renewable Hybrid Energy System Studies; Facility Design Description and Status Report*, INL/EXT-17-43269. 2017.
2. Edwards, J.N., *Thermal energy storage for nuclear power applications*. 2017, Kansas State University.
3. Anderson, R., et al., *Experimental results and modeling of energy storage and recovery in a packed bed of alumina particles*. Applied Energy, 2014. **119**: p. 521-529.
4. SOLUTIA Inc., <http://twf.mpei.ac.ru/TTHB/HEDH/HTF-66.PDF>.
5. Munro, R.G., *Evaluated material properties for a sintered alpha-alumina*. Journal of the American Ceramic Society, 1997. **80**(8): p. 1919-1928.
6. Pacheco, J.E., S.K. Showalter, and W.J. Kolb, *Development of a molten-salt thermocline thermal storage system for parabolic trough plants*. Journal of Solar Energy Engineering-Transactions of the Asme, 2002. **124**(2): p. 153-159.
7. Yang, X.P., et al., *Criteria for performance improvement of a molten salt thermocline storage system*. Applied Thermal Engineering, 2012. **48**: p. 24-31.
8. Van Lew, J.T., et al., *Analysis of heat storage and delivery of a thermocline tank having solid filler material*. Journal of solar energy engineering, 2011. **133**(2): p. 021003.
9. Polyanin, A.D. and V.E. Nazaikinskii, *Handbook of linear partial differential equations for engineers and scientists*. 2015: Chapman and hall/crc.
10. Bindra, H., et al., *Thermal analysis and exergy evaluation of packed bed thermal storage systems*. Applied Thermal Engineering, 2013. **52**(2): p. 255-263.
11. Zanganeh, G., et al., *Packed-bed thermal storage for concentrated solar power - Pilot-scale demonstration and industrial-scale design*. Solar Energy, 2012. **86**(10): p. 3084-3098.
12. Peiró, G., et al., *Two-tank molten salts thermal energy storage system for solar power plants at pilot plant scale: Lessons learnt and recommendations for its design, start-up and operation*. Renewable Energy, 2018. **121**: p. 236-248.